Ceramics International 42 (2016) 13291–13295

Contents lists available at ScienceDirect

Ceramics International

journal homepage: www.elsevier.com/locate/ceramint

Processing, microstructure and thermoluminescence response of biomorphic yttrium oxide ceramics

S.C. Santos *, C. Yamagata, L.L. Campos, S.R.H. Mello-Castanho

Instituto de Pesquisas Energeticas e Nucleares – IPEN, Av. Prof. Lineu Prestes 2242, Cidade Universitaria, Sao Paulo, Brazil

ARTICLE INFO

Article history:
Received 22 March 2016
Received in revised form
21 May 2016
Accepted 22 May 2016
Available online 24 May 2016

Keywords:
Yttrium oxide
Rare earths
Bio-prototyping
Thermoluminescence
Ceramic processing

ABSTRACT

The present work reports a fast-direct bio-prototyping process using Luffa Cylindrica vegetable sponge to produce biomorphic yttrium oxide ceramics with reticulated-porous architecture and thermoluminescence response. Processing parameters as rheology of yttrium oxide suspensions, bio-template surface treatment and thermal decomposition of bio-template were investigated. Shear thinning suspensions of 30 vol% yttrium oxide with apparent viscosity of 243mPa.s provided a successful impregnation of samples, whereby bio-templates with smooth ceramic layer and hierarchical reticulated architecture were formed. By thermal treatment at 1600 °C for 2 h biomorphic yttrium oxide ceramics with porous microstructure and TL response at 150 °C and $\lambda = 550$ nm were produced. The proposed fast-direct bio-prototyping process is suitable for the production of ceramic components with complex shape and demonstrates potential for general applicability to any bio-template.

1. Introduction

The use of renewable materials instead of those environmentally hazardous represents an essential action towards green economy and social technology [1–3]. Vegetable fibers are abundant, exhibit complex hierarchically built shape and fibrous architecture that is very promising to form functional materials.

Vegetable fibers have been very used as reinforcement in composite materials as polypropylene[4], polyester [5], epoxy [6], starch-gelatin polymer [7], poly(ethylene-*co*-vinyl acetate) [8]. Moreover, many approaches have been proposed to develop advanced ceramics by replica, sacrificial template and direct foaming [9–12]. Sugimoto et al. [13] using a cost effective method via facile electrospinning produced bio-compatible cellulose nanofibers doped with light emitting silicon nanocrystals and Au nanoparticles, improving plasmon-enhanced photoluminescence of fibers by a factor of 2.2. Santos et al. [14] by bio-prototyping of a vegetable sponge produced dysprosium doped yttrium disilicate burner with radiant efficiency of 13% and thermoluminescence response with TL peak recorded at 180 °C and wavelength of 580 nm.

Replica method consists in the impregnation of a cellular structure (wood [15], carbon sponge [16], polyurethane foam [17], vegetable sponge [18] and others natural fibers [19]) with a ceramic suspension or a precursor solution to form a reticulated ceramic alike the original template. This method is followed by high temperature thermal treatment in order to burn out the template and consolidate the ceramic phase [20]. In this method two aspects are very important, (1) the ceramic suspension has to present shear thinning behavior [21] in order to cover uniformly the template surface, (2) the thermal treatment of the impregnated template has to be performed slowly. As a result, the organic template is burned out without disrupting the ceramic structure.

Among vegetable structures, the sponge gourd of Luffa Cylindrica [22] exhibits a 3D cellular architecture being a promising shape for gas burner design, fuel filters, heat exchangers and radiation dosimeters. In addition, yttrium oxide (Y_2O_3) is a promising ceramic material for radiation dosimetry due to its luminescence, thermal, chemical, mechanical and physical proprieties[23–26]. Although Y_2O_3 has been used as a matrix for rare earth phosphors, there is a lack of studies on processing and shaping of Y_2O_3 based materials. Therefore, the present work describes a bio-prototyping process to obtain biomorphic yttrium oxide ceramics. In addition, the thermoluminescence response of Y_2O_3 is evaluated. The promising results may lead to the development of dosimetric yttrium oxide based materials.

2. Experimental

2.1. Biotemplate processing and characterization

Brazilian vegetable sponge gourd Luffa Cylindrica (LCy) was selected as bio-template of biomorphic ceramics. LCy fibers were

* Corresponding author.
E-mail address: silas.cardoso@usp.br (S.C. Santos).

http://dx.doi.org/10.1016/j.ceramint.2016.05.136
0272-8842/

cleaned by alkali treatment with 2 wt% NaOH at 60 °C for 2 h [27], seeing that some substances on fiber surface as gum and wax inhibit adhesion of other materials. As alkali treated LCy fibers were characterized by following techniques: Scanning electron microscopy (SEM, TM3000 Hitachi, Japan); thermal gravimetrical and differential thermal analyses (TGA/DTA, Setaram S60/38336, France), using a thermocouple Pt/Rth, heating rate of 10 °C min^{-1} up to 800 °C in air; X-ray diffraction (XRD, Rigaku Multiflex, Japan), with an angular range (2θ) from 20 to 80°, scanning of 0.5° min^{-1} and Kα source, followed by determination of the index of crystallinity (CI_{XRD}) using the peak height method [28] as shown in Eq. (1); Fourier transform infrared spectroscopy (FTIR, Thermo Nicolet iS50), followed by determination of the index of crystallinity (CI_{FTIR}) using Nelson et al. [29] model as shown in Eq. (2).

$$CI_{XRD}=\left[\frac{(I_{022}-I_{am})}{I_{022}}\right].100\,[\%] \quad (1)$$

$$CI_{FTIR}=\left(\frac{a_{1372}}{a_{2900}}\right)[a.u] \quad (2)$$

where a_{1372} and a_{2900} are the absorbance intensities of the bands at 1372 and 2900 cm^{-1} for O–H bending and C–H stretching, in FT-IR spectra respectively.

2.2. Ceramic powder, irradiation and TL response

Rare earth C-type yttrium oxide powders (Y_2O_3, 99.9%, Alfa Aesar GmbH & Co. KG), with mean particle size (d_{50}) of 304 nm, pycnometric density (ρ) of 4.84 g cm^{-3} and specific surface area (SSA) of 6.4 m^2 g^{-1} were used as raw material.

Yttrium oxide powders were irradiated with 10 kGy dose using gamma cell source at Instituto de Pesquisas Energéticas e Nucleares (IPEN), Sao Paulo, Brazil. Thermoluminescence response (TL) of Y_2O_3 particles was performed on a thermoluminescence reader (Risø TL/OSL-DA-20) based on a heating rate of 2 °C s^{-1} up to 400 °C in a nitrogen atmosphere and a spectrometer (Ocean Optics, model QE65 Pro) with spectral sensitivity from 200 to 950 nm.

2.3. Preparation of ceramic suspension and flow characterization

The study on stabilization of Y_2O_3 suspensions is reported in our previous work [30]. Therefore, all parameters described here are optimized. Aqueous Y_2O_3 suspensions with 30 vol% solids content were prepared using tetramethylammonium hydroxide (TMAH, Sigma-Aldrich), 1 wt% ammonium poly acrylic acid (PAA, Sigma-Aldrich), and 0.3 wt% carboxymethyl-cellulose (CMC, Sigma-Aldrich). The homogenization of suspensions was performed in a ball mill for 24 h using alumina spheres ($Ø_{spheres}$ = 10 mm).

The flow behavior of Y_2O_3 suspensions was evaluated using a rheometer (Haake RS600, Thermo Scientific) with a double-cone rotor and a stationary plate (DC60/1°). The flow behavior of the suspensions was characterized in the control rate mode (CR) and compared with rheological models available in rheometer database (Haake Rheowin Data Manager v. 3.61.0.1). All measurements were evaluated at 25 °C, shear rate ($\dot{\gamma}$) from 0 to 1000 s^{-1} in 5 min, holding for 2 min at 1000 s^{-1} and returning to 0 s^{-1} in 5 min. For each CR step 200 points were measured.

2.4. Bio-prototyping and characterization of biomorphic yttrium oxide ceramics

Biomorphic Y_2O_3 ceramics were shaped by bio-prototyping. LCy samples (40 × 45 × 30 mm) were immersed in Y_2O_3 suspension for 30 min (optimized time) [31]. The excess of ceramic suspension was removed by squeezing out the samples for three times. As impregnated LCy samples were dried at environmental temperature for 24 h, followed by sintering at 1600 °C for 2 h in air using a vertical furnace (Lindberg/Blue M).

Microstructural analyses on grain size-shape, porous distribution, fracture surface and reticulated architecture of the sintered biomorphic yttrium oxide ceramics were performed with an optical microscope (Jena GSZ, Carl Zeiss) and by SEM.

3. Results and discussion

Vegetable fibers presents as characteristic light weight, high specific surface area, significant architecture and promising applicability to new materials. As illustrated in Fig. 1a and b LCy fibers form a reticulated architecture, which is supported by struts. The strength of struts is ascribed to its fibrils glued together with natural resinous materials of plant tissue. As a result, the natural mat of LCy exhibited pycnometric density (ρ) of 1.55 g cm^{-3} and specific surface area (SSA) of 22.5 m^2 g^{-1} (Fig. 1a). Although high specific surface are is a general characteristic of LCy fibers, surface substances may inhibit impregnation of ceramic suspension and a chemical treatment is necessary to clean LCy fibers surface. Thus, NaOH solutions are usually used to remove these substances and to prepare the surface of fiber for impregnation. As a consequence of the alkaline treatment, fibers exhibited scratches on the surface due to removal of the lining and hemicellulose. In addition, hollow micro channels from plant tissue became visible. Hence, the alkaline treatment with 2 wt% NaOH at 60 °C for 2 h was cost-effective to clean the surface of LCy fibers and to enhance the impregnation of ceramic suspension.

Fig. 2 illustrates FT-IR spectra of LCy fibers (a) in nature and (b) treated with 2 wt%NaOH. The vibrational bands at 3416, 2916, 1638, 1417, 1323, 1161, 1046, and 895 cm^{-1} are associated to native cellulose [32] for both samples. LCy fibers in nature exhibited intense characteristic peaks at 1595 cm^{-1} (free hydroxyl band), 1740 cm^{-1} (acid carbonyl absorption), 2750–2800 cm^{-1} (typical CH_2 and CH), 3200–3300 cm^{-1} (the O–H stretching band), 1100 cm^{-1} (C–O–C absorption), and 1000–1500 cm^{-1} (the aromatic region related to the lignin). For LCy fibers treated with 2 wt% NaOH no strong absorption at 1735 cm^{-1} (the carboxyl group: –O–CaO) was observed. On the other hand, a band reduction at 1245 cm^{-1}(C–H) was identified. The peak for O-H stretching is an indicative of the brake of hydrogen bonds in

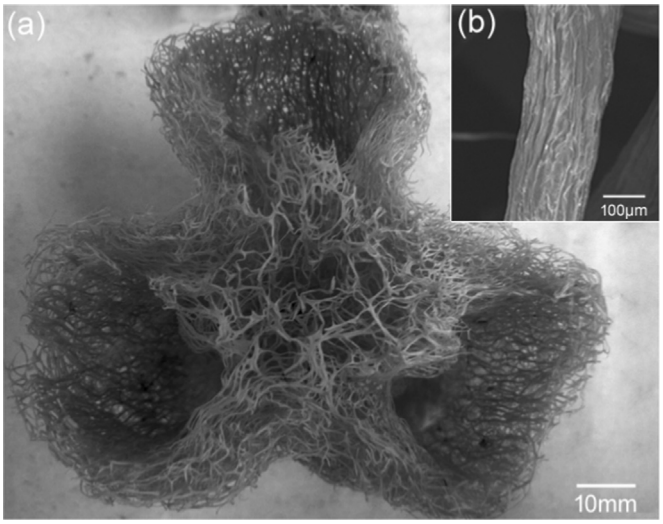

Fig. 1. Vegetable sponge Luffa Cylindrica (LCy). (a) optical image of the natural mat; (b) SEM image of fiber after alkali treatment.

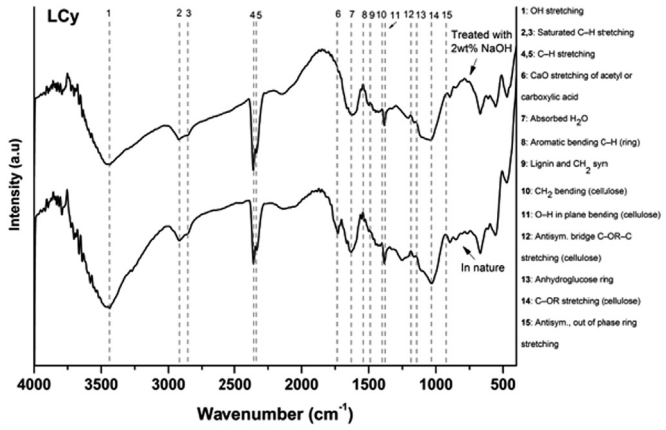

Fig. 2. FT-IR spectra of LCy as (a) in nature and (b) treated with 2 wt% NaOH.

cellulose. In addition, the peak for CH_2 bending shifted to a lower frequency from 1431 cm^{-1} to 1419 cm^{-1}, which was a hint for the splitting of hydrogen bonds in C_6-OH [33]. Furthermore, the alkaline treatment used to remove surface impurities of LCy fibers led to increase of N_O'KI index from 0.8842 to 1.0694, which represents the relative changes of cellulose crystallinity [34,35].

The production of a ceramic component by bio-prototyping requires the knowledge on thermal decomposition behavior of the biotemplate, which in turn implies on thermal treatment of the ceramic component. Fig. 3 illustrates the thermal decomposition behavior of the LCy template by TGA/TDG analyses. Black thick line represents TGA curve, light grey line illustrates TDG curve and dark grey line is the derivate of TGA, DTG. TGA curve exhibits distinct decomposition regions, loss of water at 100 °C, hemicellulose degradation from 100 to 280 °C, cellulose degradation from 260 to 350 °C and lignin degradation from 350 to 500 °C. From DTG curve (dark grey line) is observed the maximum decomposition peak of substances. A critical zone, which corresponds to a substantial loss of weight (76 wt%) took place between 250 °C and 450 °C and from 500 °C the LCy structure was totally burned out (100 wt%). As can be seen, the knowledge of decomposition behavior of the template as a function of temperature is primary to define a thermal treatment. Furthermore, a well-controlled thermal treatment is fundamental to produce biomorphic ceramics. Based on results the following conditions of thermal treatment of impregnated samples was set as a heating rate of 1 °C min^{-1} up to 1600 °C for 2 h in air.

Vegetable fibers exhibit substantial crystallinity, which is associated to cellulose content. As illustrated in Fig. 4a LCy fibers in

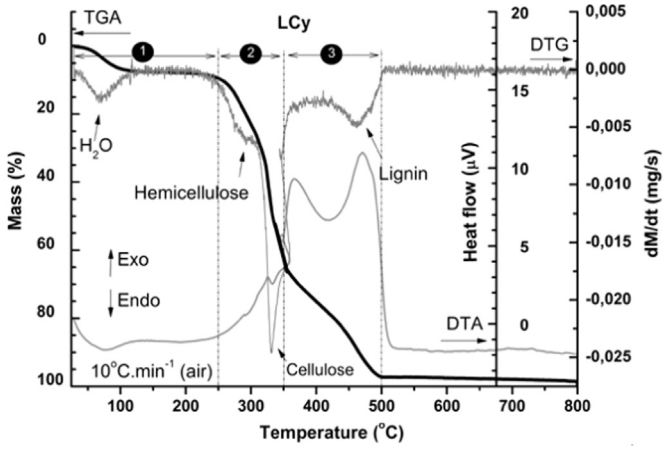

Fig. 3. Thermal analysis (TGA/DTA/DTG) of LCy fibers at 10 °C min^{-1} up to 800 °C in air.

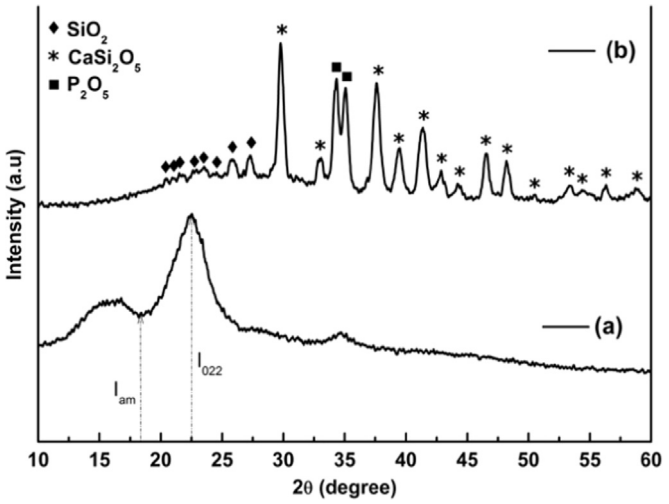

Fig. 4. X-ray diffraction curves (XRD) of (a) in nature LCy fibers and (b) ashes from LCy fibers after calcination at 800 °C for 1 h in air.

nature exhibited a wide peak around of 23°, which indicates a short crystalline arrangement order due to cellulose [36]. The hydroxyl groups contain macromolecules involved in a number of intra-and intermolecular hydrogen bonds, which result in various ordered crystalline arrangements in cellulose. The maximum peak was around of 23° and corresponded to the plane (022), I_{022}. On the other hand, the peak which corresponds to amorphous structure was around of 18° and its intensity was set as $I_{am.}$ From these parameters the estimative of the crystallinity index (CI_{XRD}) was of 44%. According to Fig. 4b, the ashes formed from calcination at 800 °C are based on inorganic substances such as, Na, Mg, K, P, Ca, Cl, SiO_2 and silicates [35,37], which are from plant tissue and soil. From Fig. 4b diffraction peaks were identified for the compounds $CaSi_2O_5$ (30, 33, 36-60°; PDF. 51-92), SiO2 (21-29°; PDF. 14-260) and P_2O_5 (34,35°; PDF. 83-602).

The thermoluminescence (TL) response curve of yttrium oxide nanoparticles is shown in Fig. 5. As seen in Fig. 5a, yttrium oxide exhibited a TL peak at 150 °C and light emission quanta at 550 nm. TL process can be divided into three basic steps as shown in Fig. 5b: (1) creation of free charges by ionizing radiation (I_R); (2) trapping of free charges and (3) lighting emission as thermally stimulated. The use of ionizing radiation (1) leads to dislocation of electrons from the valence band (VB) to reach the conduction band (CB) and are trapped (2) at the trapping electron center (T). Meanwhile, vacancies from VB go through the crystal lattice until be trapped at the trapping vacancy center (R). As the solid is heated and the temperature reaches a value in which the thermal vibration is suitable to lead to liberation of electrons from (T), these electrons can reach the recombination center (R). The result of the recombination of electrons and vacancies is an emission of a visible light (3).

This particular luminescence response observed at 550 nm for yttrium oxide nano particles is new in literature (Fig. 5a). Although the high energetic gamma beam creates more number of oxygen vacancies which are related to the F and F+ centers, there is evidence that the TL response of yttrium nano particles is also attributed to its chemical composition, crystal lattice and crystal defects. These factors can produce charge-carrier vacancies and luminescence centers. Raukas et al. [38] reported that yttrium oxide nanoparticles exhibited white light luminescence at 330 nm like Y_2O_3:Ce^{3+}. Bordun [39] suggested that the luminescence bands with λ maxima at 365 and 428 nm are ascribed to the presence of oxygen vacancies associated to radiative recombination process. Osipov et al. [40] described that yttrium oxide

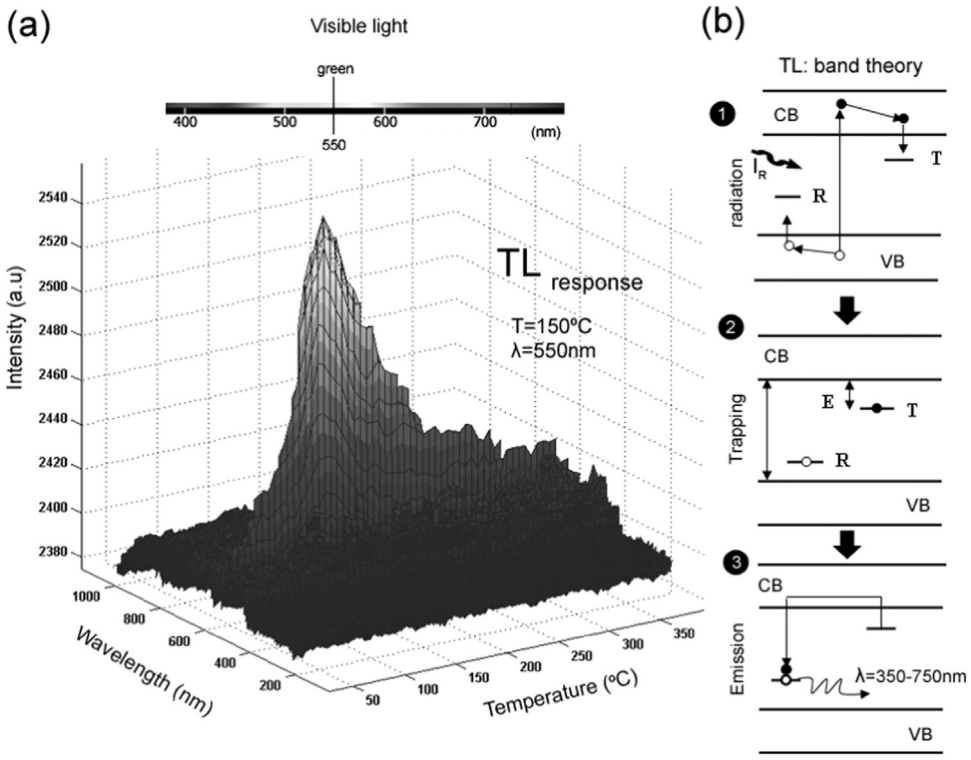

Fig. 5. (a) TL response of Y_2O_3 particles at 150 °C and λ of 550 nm. (b) radiation-trapping-emission process in a solid structure from band theory, in which I_R: irradiation; CB: conduction band, VB: valence band, T: trapping electron center; R: recombination center; black circles represent electrons, whereas light ones the holes.

cathodoluminescence spectra with peak at 465 nm was due to recombination of associative Y^{3+}–O^{2-} donor acceptor pair. Therefore, it is assumed that this material contain intrinsic luminescence centers.

The flow curves of 30 vol% suspensions of Y_2O_3 in CR mode are illustrated in Fig. 6a. From stress curves (square symbol) is observed a significant area between up and down curves due to particle characteristics as size and shape, which lead to formation of agglomerates. This behavior known as thixotropy can also be associated with extension of polymer chains, particles deformation, and break down of particle agglomerates formed by binder and others polymeric additives. The present shear curves exhibited thixotropy of $.394.10^6$ Pa s^{-1}.

For viscosity flow curves (circle symbol) shear thinning behavior, in which apparent viscosity (η) decreases as the shear rate ($\dot{\gamma}$) increases, is observed. Some unstable flow is noted for $\dot{\gamma} < 100\ s^{-1}$, as the condition of ceramic suspension changes from static to dynamic (flowing), which ascribes that the structure of ceramic suspension is modified as a function of shear rate. Thus, the stability and particle characteristics define the rheology of suspension. As a result, the flow behavior of 30 vol% Y_2O_3 suspension in CR mode fitted to Cross model and the following parameters were determined, initial viscosity (η_0) of 5.848 mPa s; infinite viscosity (η_∞) of 44.85 mPa s; shear rate ($\dot{\gamma}$) of 2.569 s^{-1} and index (n) of 1.707.

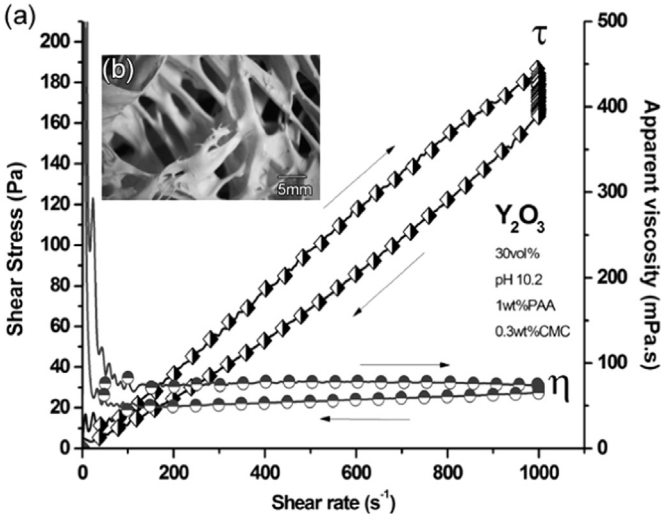

Fig. 6. (a) Flow curves of Y_2O_3 suspensions in CR mode; (b) optical image of LCy sample impregnated using this suspension.

Based on our previous experiences [41–43], for replica method is desirable that ceramic suspensions exhibit viscosity less than 800 mPa s, once high viscous suspensions do not impregnate suitably template surface. Besides, viscous suspensions provide poor coating, filled traps, high roughness, deformation and shaping defects. In the present study Y_2O_3 suspension exhibited apparent viscosity at 10 s^{-1} of 243 mPa s. As a result, the suspension was like an ink and promoted a smooth layer on LCy template as illustrated in Fig. 6b.

The optical image of the sintered biomorphic yttrium oxide ceramic is shown in Fig. 7a. High thermal temperature treatment at 1600 °C for 2 h led to formation of ceramic body with reticulated architecture and biomorphic shape. As a result, the biomorphic ceramic exhibited loss weight of 6% and pycnometric density of 4.55 g cm^{-3} (90% theoretical density). Ceramic fibers (Fig. 7b), which are composed of at least two hollows with inner diameter higher than 50 μm exhibited dense microstructure with heterogeneous distribution of grains size-shape. In addition, fracture fibers showed cleavage planes, some closed porous and transgranular fracture.

4. Conclusion

In the present work a biomorphic yttrium oxide ceramic with reticulated architecture and thermoluminescent response at

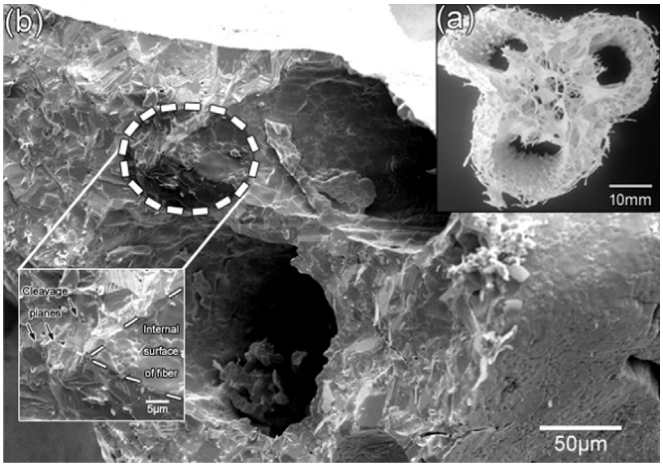

Fig. 7. (a) Optical image of biomorphic yttrium oxide ceramic produced by bio-prototyping, (b) SEM image of the fracture ceramic fiber showing its inner microstructure, hollows and cleavage planes.

150 °C and 550 nm was developed by bio-prototyping from the vegetable sponge Luffa Cylindrica. Shear thinning suspensions with suitable apparent viscosity were prepared with 30 vol% solid content, pH of 10.2, 1 wt% dispersant and 0,3 wt% binder. Alkali treatment of the vegetable fibers with 2 wt% NaOH at 60 °C for 2 h was useful to prepare the biotemplating surface for replica method. Thermal treatment at 1600 °C for 2 h in air enabled the production of biomorphic yttrium oxide ceramics with dense microstructure and pycnometric density of 4.23 g cm^{-3} (90% theoretical density).

Acknowledgments

We authors are deeply grateful to Dr. Thomaz Augusto Restivo, Dr. Linda Caldas, Dr. Maira Tiemi Yoshizumi, Dr. Francisco Braga, MSc. Douglas Will Leite, and MSc. William Naville. In addition, Grant #2014/23621-3 from São Paulo Research Foundation (FAPESP); National Council for Scientific and Technological Development (CNPq), and Coordination for Improvement of High Degree People (CAPES).

References

[1] R. Melendez-Ortiz, Governance of international trade for the green economy, Rev. Policy Res. 28 (2011) 479–486.
[2] F. Bran, I. Ioan, C.V. Radulescu, A. Pana, Towards sustainable development via a green economy, Innovation and Knowledge Management: A Global Competitive Advantage, vol. 1–4, 2011, pp. 644–649.
[3] D.J. Hess, Publics as threats? Integrating science and technology studies and social movement studies, Sci. Cult. 24 (2015) 69–82.
[4] R. Eslami-Farsani, Effect of fiber treatment on the mechanical properties of date palm fiber reinforced PP/EPDM composites, Adv. Compos. Mater. 24 (2015) 27–40.
[5] P. Georgiopoulos, E. Kontou, The effect of wood-fiber type on the thermomechanical performance of a biodegradable polymer matrix, J. Appl. Polym. Sci. 132 (2015) 15.
[6] R. Prithivirajan, S. Jayabal, G. Bharathiraja, Bio-based composites from waste agricultural residues: mechanical and morphological properties, Cellul. Chem. Technol. 49 (2015) 65–68.
[7] W. Rodriguez-Castellanos, F.J. Flores-Ruiz, F. Martinez-Bustos, F. Chinas-Castillo, F. J. Espinoza-Beltran, Nanomechanical properties and thermal stability of recycled cellulose reinforced starch-gelatin polymer composite, J. Appl. Polym. Sci. 132 (2015).
[8] C.J. Tan, J. Peng, W.H. Lin, Y.X. Xing, K. Xu, J.C. Wu, et al., Role of surface modification and mechanical orientation on property enhancement of cellulose nanocrystalsi-polymer nanocomposites, Eur. Polym. J. 62 (2015) 186–197.
[9] J.W. Li, S.Q. Yu, M. Ge, X. Wei, Y.B. Qian, Y. Zhou, et al., Fabrication and characterization of biomorphic cellular C/SiC-ZrC composite ceramics from wood, Ceram. Int. 41 (2015) 7853–7859.
[10] T. Zhang, Y.M. Zhou, M. He, X.H. Bu, Y.J. Wang, C. Zhang, Templated fabrication of biomorphic alumina-based ceramics with hierarchical structure, J. Eur. Ceram. Soc. 35 (2015) 1337–1341.
[11] B. Matovic, D. Nikolic, N. Labus, S. Ilic, V. Maksimovic, J. Lukovic, et al., Preparation and properties of porous, biomorphic, ceria ceramics for immobilization of Sr isotopes, Ceram. Int. 39 (2013) 9645–9649.
[12] A.R. Studart, U.T. Gonzenbach, E. Tervoort, L.J. Gauckler, Processing routes to macroporous ceramics: a review, J. Am. Ceram. Soc. 89 (2006) 1771–1789.
[13] H. Sugimoto, R. Zhang, B.M. Reinhard, M. Fujii, G. Perotto, B. Marelli, et al., Enhanced photoluminescence of Si nanocrystals-doped cellulose nanofibers by plasmonic light scattering, Appl. Phys. Lett. 107 (2015) 041111.
[14] S.C. Santos, C. Yamagata, L.L. Campos, S.R.H. Mello-Castanho, Processing and thermoluminescent response of porous biomorphic dysprosium doped yttrium disilicate burner, Mater. Chem. Phys. 177 (2016) 505–511.
[15] Z.T. Liu, T.X. Fan, W. Zhang, D. Zhang, The synthesis of hierarchical porous iron oxide with wood templates, Microporous Mesoporous Mater. 85 (2005) 82–88.
[16] A.J. Sherman, R.H. Tuffias, R.B. Kaplan, Refractory ceramic foams – a novel, new high-temperature structure, Am. Ceram. Soc. Bull. 70 (1991) 1025–1029.
[17] J. Luyten, I. Thijs, W. Vandermeulen, S. Mullens, B. Wallaeys, R. Mortelmans, Strong ceramic foams from polyurethane templates, Adv. Appl. Ceram. 104 (2005) 4–8.
[18] S.A. Silva, D.D. Brunelli, F.C.L. Melo, G.P. Thim, Preparation of a reticulated ceramic using vegetal sponge as templating, Ceram. Int. 35 (2009) 1575–1579.
[19] B. Ben-Nissan, Natural bioceramics: from coral to bone and beyond, Curr. Opin. Solid State Mater. Sci. 7 (2003) 283–288.
[20] J. Luyten, S. Mullens, J. Cooymans, A.M. De Wilde, I. Thijs, R. Kemps, Different methods to synthesize ceramic foams, J. Eur. Ceram. Soc. 29 (2009) 829–832.
[21] R. Moreno, Reología ae Suspensiones Cerámicas, Consejo Superior De Investigaciones Científicas, Madrid, 2005.
[22] A. Shahidi, N. Jalilnejad, E. Jalilnejad, A study on adsorption of cadmium(II) ions from aqueous solution using Luffa cylindrica, Desalination Water Treat. 53 (2015) 3570–3579.
[23] V. Solomonov, V. Osipov, A. Spirina, Luminescence of Yb-doped YAG: divalent ytterbium ions, J. Lumin. 169 (2016) 151–155.
[24] M.A. Auger, V. de Castro, T. Leguey, J. Tarcisio-Costa, M.A. Monge, A. Munoz, et al., Effect of yttrium addition on the microstructure and mechanical properties of ODS RAF steels, J. Nucl. Mater. 455 (2014) 600–604.
[25] J. Hostasa, J. Matejicek, B. Nait-Ali, D.S. Smith, W. Pabst, L. Esposito, Thermal properties of transparent Yb-doped YAG ceramics at elevated temperatures, J. Am. Ceram. Soc. 97 (2014) 2602–2606.
[26] J.S. Souris, S.H. Cheng, C. Pelizzari, N.T. Chen, P. La Riviere, C.T. Chen, et al., Radioluminescence characterization of in situ x-ray nanodosimeters: potential real-time monitors and modulators of external beam radiation therapy, Appl. Phys. Lett. 105 (2014).
[27] V.O.A. Tanobe, T.H.D. Sydenstricker, M. Munaro, S.C. Amico, A comprehensive characterization of chemically treated Brazilian sponge-gourds (Luffa cylindrica), Polym. Test. 24 (2005) 474–482.
[28] L. Segal, J.J. Creely, A.E. Martin, C.M. Conrad, An empirical method for estimating the degree of crystallinity of native cellulose using the X-ray diffractometer, Text. Res. J. 29 (1959) 786–794.
[29] M.L. Nelson, R.T. O'Connor, Relation of certain infrared bands to cellulose crystallinity and crystal latticed type. Part I. Spectra of lattice types I, II, III and of amorphous cellulose, J. Appl. Polym. Sci. 8 (1964) 1311–1324.
[30] S.C. Santos, W. Acchar, C. Yamagata, S. Mello-Castanho, Yttria nettings by colloidal processing, J. Eur. Ceram. Soc. 34 (2014) 2509–2517.
[31] S.C. Santos, C. Yamagata, W. Acchar, S.R.H.M. Castanho, Yttria nettings by replica processing, Mater. Sci. Forum 798 (2014) 3.
[32] C.F. Liu, R.C. Sun, J. Ye, Structural and thermal characterization of sugarcane bagasse phthalates prepared with ultrasound irradiation, Polym. Degrad. Stab. 91 (2006) 280–288.
[33] H. Zhang, J. Wu, J. Zhang, J.S. He, 1-Allyl-3-methylimidazolium chloride room temperature ionic liquid: a new and powerful nonderivatizing solvent for cellulose, Macromolecules 38 (2005) 8272–8277.
[34] M. Adam, M. Oschatz, W. Nickel, S. Kaskel, Preparation of hierarchical porous biomorphic carbide-derived carbon by polycarbosilane impregnation of wood, Microporous Mesoporous Mater. 210 (2015) 26–31.
[35] A.D. French, M.S. Cintron, Cellulose polymorphy, crystallite size, and the Segal Crystallinity Index, Cellulose 20 (2013) 583–588.
[36] S. Park, J.O. Baker, M.E. Himmel, P.A. Parilla, D.K. Johnson, Cellulose crystallinity index: measurement techniques and their impact on interpreting cellulase performance, Biotechnol. Biofuels 3 (2010).
[37] B.L. Browning, The Chemistry of Wood, Interscience, New York, 1963.
[38] M. Raukas, A. Konrad, K.C. Mishra, Luminescence in nano-size Y_2O_3:Ce, J. Lumin. 122–123 (2007) 773–775.
[39] O.M. Bordun, Influence of oxygen vacancies on the luminescence spectra of Y_2O_3 thin films, J. Appl. Spectrosc. 69 (2002) 430–433.
[40] V.V. Osipov, A.V. Rasuleva, V.I. Solomonov, Luminescence of pure yttria, Opt. Spectrosc. 105 (2008) 524–530.
[41] S.C. Santos, C. Yamagata, L.L. Campos, S.R.H. Mello-Castanho, Bio-prototyping and thermoluminescence response of cellular rare earth ceramics, J. Eur. Ceram. Soc. 36 (2016) 791–796.
[42] S.C. Santos, C. Yamagata, A.C. Silva, L.F.G. Setz, S.R.H. Mello-Castanho, Yttrium disilicate micro-cellular architecture from biotemplating of Luffa cylindrica, J. Ceram. Sci. Technol. 5 (2014) 203–208.
[43] S.C. Santos, C. Yamagata, W. Acchar, S.R.H. Mello-Castanho, Yttria nettings by replica processing, Brazilian Ceramic Conference 57, vol. 798–799, 2014, pp. 687–690.